

# A multidisciplinary study on the spatial variability of the local stratigraphic conditions in partially saturated slopes for flow-like landslide prediction

Marianna Pirone<sup>1\*</sup>, Rosa Di Maio<sup>2</sup>, Giovanni Forte<sup>1</sup>, Claudio De Paola<sup>2</sup>, Simona Guglielmi<sup>3</sup>, Rosanna Salone<sup>2</sup>, Antonio Santo<sup>1</sup>, Gianfranco Urciuoli<sup>1</sup>

<sup>1</sup> Dipartimento di Ingegneria Civile, Edile e Ambientale, Università degli Studi di Napoli Federico II, Naples, Italy

<sup>2</sup> Dipartimento di Scienze della Terra, dell'Ambiente e delle Risorse, Università degli Studi di Napoli Federico II, Naples, Italy

<sup>3</sup> Formerly Scuola Superiore Meridionale, Largo S. Marcellino, 10, 80138 Napoli, Italy

**Abstract.** Flow-like landslides, which occur mainly in shallow granular deposits resting on steep bedrock, represent a major natural hazard worldwide. The pore water pressure distribution and the soil water content directly affect the soil shear strength, thus controlling the triggering of these landslides. Critical geomorphological and topographical settings, together with peculiar stratigraphic and hydrogeological features, are commonly recognized as predisposing factors for flow-like landslides occurrence. Hence, investigating the spatial and temporal variability of hydraulic slope conditions is a fundamental activity that consists of identifying local geological factors and seasonal monitoring of the subsurface water regime. The present work proposes an integrated geological, geophysical and geotechnical approach to identify the spatial variability of the local stratigraphic setting and hydrogeological conditions in a partially saturated slope, in order to set up a procedure able to provide a prediction of the flow-like landslides occurrence at slope scale. The multidisciplinary study has been applied to a test site on Mt. Faito, in the Lattari Mts. (Southern Italy), where extensive geophysical, geological and geotechnical soil characterization and in situ monitoring data collected over two years are available.

## 1 Introduction

Geomorphological, topographical, stratigraphic and hydrogeological characteristics of a slope are commonly recognized as predisposing factors for flow-like landslides (flowslides, debris flows and debris avalanches), which occur mainly in shallow granular deposits resting on steep bedrock [1-4]. In this regard, the influence of the irregularities of these features on slope stability is crucial for shallow landslides (a few tens/hundreds of cubic metres), for which detailed information at the scale of metres or tens of metres is required. Despite advances made in field testing, the collection of exhaustive data is still a challenge. While geological and geotechnical investigation methods provide detailed information at point locations, soil formations can be highly variable in space. In this framework, geophysical surveys can provide continuous spatial insights by developing 2D or 3D subsurface models in terms of physical parameters closely linked to soil properties, such as lithology, porosity, saturation degree and stress state [5-8].

The present study proposes an integrated geological, geophysical and geotechnical approach to identify the spatial variability of the local stratigraphic setting and hydrogeological conditions in partially saturated slopes.

The overall goal is to detect local stratigraphic features affecting the area in terms of geometry, continuity and thickness of soil horizons, and then to investigate their influence on the groundwater regime over time. In this way, irregularities relevant to slope stability are individuated and the critical areas where flow-like landslides could be triggered at the slope scale can be identified, thus improving the predictive capacity of Early Warning Systems.

The proposed multidisciplinary study has been applied to a test site on Mt. Faito, in the Lattari Mts. (Southern Italy), where extensive geological and geotechnical soil characterization was carried out and in situ monitoring data of matric suction, subsurface volumetric water content and meteorological data were collected over two years [9-11]. In particular, the results of 2D/3D Electrical Resistivity Tomography (ERT) surveys along parallel profiles in the test area were integrated with geological and geotechnical investigations to determine the electro-stratigraphic and geological setting of the cover, the local morphology and the physical conditions of the underlying bedrock. In addition, 3D models of the effective saturation degree in different pyroclastic horizons were retrieved thanks to characteristic curves of electrical resistivity vs saturation degree determined by laboratory

---

\* Corresponding author: [marianna.pirone@unina.it](mailto:marianna.pirone@unina.it)

measurements on samples from the investigated soil layers [1]. The spatial distribution model of volumetric water content was validated by comparing water contents measured along vertical profiles by TDR (Time Domain Reflectometry) probes and those obtained from field resistivity measurements. Finally, 3D ERT surveys carried out in two different seasonal periods, summer and winter, along one of the investigated profiles, are shown to infer the time evolution of the groundwater flow-paths at the slope scale.

## 2 Multidisciplinary study

The observation of many flow-like landslides in Campania has clearly shown that the trigger is caused by local slope conditions, recognized as predisposing factors, which can vary over a wide range, resulting in several possible unfavourable combinations [12-14]. Buried predisposing factors include: i) critical geomorphological and stratigraphic contacts between shallower soils and bedrock; ii) nearly impermeable layers consisting of clayey ashes sealing the fractured bedrock beneath the pyroclastic soils; iii) preferential rainwater infiltration pathways consisting of zones of higher permeability; and iv) springs feeding the surficial pyroclastic cover. The proposed multidisciplinary study fits within this framework, as the approach herein discussed contributes to a spatial prediction of flowslide occurrence.

First, the results of a 2D ERT survey along parallel profiles in the test area are integrated with geological observations and geotechnical investigations carried out on soil samples which are representative of the surveyed slope to determine: i) the electro-stratigraphic and geological setting of the cover, ii) the local morphology and iii) the physical conditions of the underlying bedrock.

Then, a high-resolution 3D ERT survey is performed to obtain a detailed geometric and physical characterization of the whole pyroclastic cover volume in terms of water content distribution. The obtained model is then validated by comparing the water contents measured along some vertical profiles by TDR probes with those obtained from field resistivity measurements, thus calibrating the spatial model of the water content distribution. The scheme of the multidisciplinary approach followed is shown in Fig. 1.

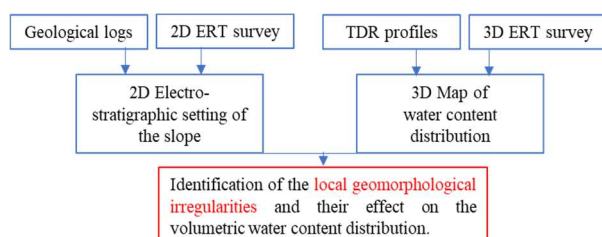


**Fig. 1.** Scheme of the multidisciplinary approach to identify predisposing factors for flow-like landslide occurrence.

## 3 Application of the multidisciplinary approach

### 3.1 Test site

The multidisciplinary study was developed for the Mt. Faito test site (Lattari Mts., Campania region in southern Italy) [1,13] and both field and laboratory data were adopted.

The test site was chosen for the presence of the main geological and stratigraphic features significant for the initiation of flow-like landslides. The area lies between 826 and 870 m above sea level (a.s.l.) on the northern slope of Mt. Faito in the municipality of Castellammare di Stabia (Naples) (Fig. 2a) (modified from [1]). The area is characterized by a fractured and karst limestone bedrock covered by pyroclastic soils 1–2 m thick and slope angles between 27° and 35°, which are the most critical for triggering such landslides.

### 3.2 Geological setting

The stratigraphic setting was reconstructed from 21 stratigraphic logs. The geological survey helped to determine the general attitude of the bedding, along with the fractured and karst part of the bedrock. The local stratigraphic setting is shown in Fig. 2c. The two uppermost layers, i.e., A1 (20–30 cm thick) and A2 (40–100 cm thick), originated from the 79 A.D. eruption and define the upper portion of the soil. These layers can be classified as silty sand with gravel (A1) and silty gravel with sand (A2). The stratigraphic sequence of this eruption is opened by the B layer, formed by well-graded white pumice (2–4 cm in diameter) in a thin sandy pyroclastic matrix. Its thickness is strongly variable from less than 1 m to more than 2 m. The deposit of the older eruption is defined by the C1 (40–180 cm thick) and C2 (20–200 cm thick) layers, both consisting of sandy silts (Fig. 2c).

### 3.3 Geotechnical investigation

The geotechnical study consisted of both laboratory and field investigations. Soil physical properties and grain-size distribution were determined in the laboratory to confirm the stratigraphic profile established by the geological survey [10]. Then, in order to identify the hydraulic slope condition over time, seasonal variations in suction and volumetric water content were investigated by installing 40 tensiometers and 42 TDR probes in situ along 10 vertical profiles at different depths (see location in Fig. 2b).

In this paper, volumetric water content (VWC) measurements collected at fixed depth points were compared with those obtained at the same points from field resistivity measurements to validate the spatial model of water content distribution discussed in Section 3.4.

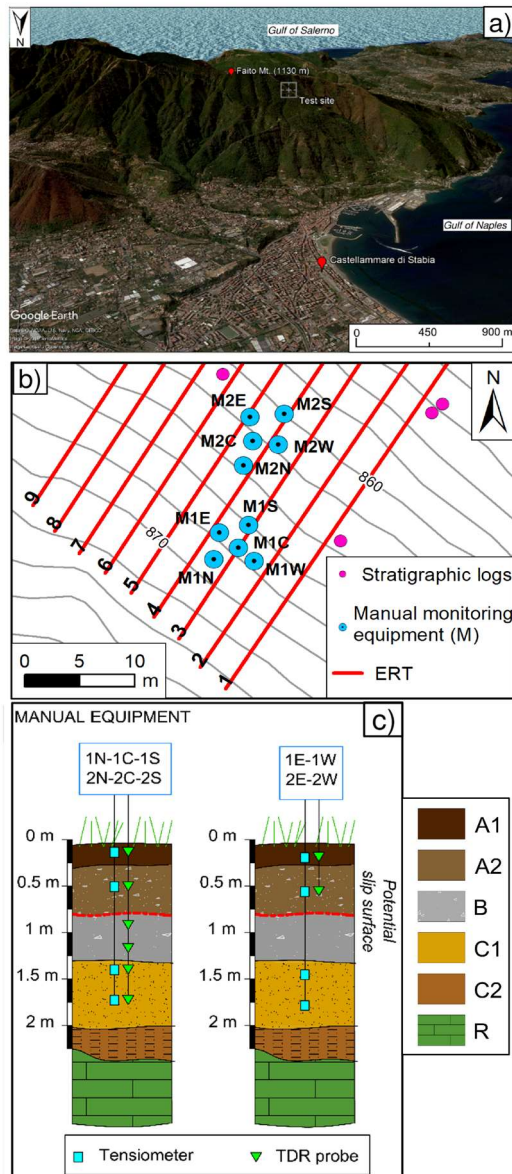


**Fig. 2.** a) Location of the test site on the Lattari Mts.; b) detail of the distribution of the ERT resistivity profiles and soil sampling sites. The blue circles indicate the position of the two parcels, 1 and 2, where TDR probes and tensiometers were installed along ten vertical sections (five per parcel) at different depths; c) stratigraphic sequence of the Lattari Mts along with the installation depth of the conventional tensiometers and TDR probes at the vertical profiles equipped with manual monitoring instruments (M) (modified after [1, 9]).

### 3.3.1 Laboratory investigation

Table 1 shows the mean values of the determined physical properties: specific gravity  $G_s$ , dry unit weight  $\gamma_d$ , soil porosity  $n$ , Atterberg Limits and saturated hydraulic conductivity,  $k_{SAT}$ . Saturated permeability tests at constant head were performed on saturated soil samples using a permeameter. Surficial soils A1, A2 and layer C1 have similar porosity values, ranging between 0.67 and 0.72. The deepest layer, C2, has a very low porosity compared to the other soils. The saturated permeability values of soils A1, A2 and C1 are

comparable with each other, ranging between  $5.0 \cdot 10^{-7}$  and  $1.0 \cdot 10^{-6}$  m/s [10,11]. In line with its very low soil porosity, the saturated permeability of C2 is two orders of magnitude lower than that of the other layers ( $6.40 \cdot 10^{-9}$  m/s). It is worth noting that the presence of the finer layer C2 at the bottom of the pyroclastic cover facilitates the increase in saturation of the overlying soils or even the occurrence of positive pore water pressure at the bottom of the soil cover during heavy rainfall in the wet period (December-May), thereby worsening the stability conditions. The Atterberg limits were achieved only for soil layer C2. Mean Atterberg limits over five determinations performed on soil layer C2 are reported in Table 1. The soil C2 can be classified as a medium plasticity silt. For further details about the soil properties recognized at the test site, the readers can refer to [10].

**Table 1.** Mean values of soil physical properties, Atterberg limits and saturated hydraulic conductivity.

Soil	$G_s$	$\gamma_d$ ( $\text{kN/m}^3$ )	$n$	WL (%)	WP (%)	$I_p$ (%)	$k_{SAT}$ (m/s)
A1	2.67	8.80	0.67	-	-	-	$4.35 \cdot 10^{-7}$
A2	2.70	8.10	0.69	-	-	-	$1.43 \cdot 10^{-6}$
C1	2.62	7.34	0.72	-	--	-	$6.62 \cdot 10^{-7}$
C2	2.65	14.18	0.46	50.7	39.6	11.1	$6.40 \cdot 10^{-9}$

### 3.3.2 Field monitoring

With regard to the field investigation, two zones were identified for the equipment installation. In each zone, five verticals were instrumented as shown in Fig. 2b; three verticals, N, C, S, are aligned along the maximum slope direction, while two verticals, W and E, are aligned along the contour lines (perpendicular to the previous alignment). In order to measure volumetric water content (VWC) and matrix suctions, TDR probes and tensiometers were installed along the five verticals at different depths (Fig. 2c). In all, 20 tensiometers and 20 TDR probes were installed in the shallowest soils, A1 and A2 (at depths between 0.2 and 0.6 m), 11 TDR probes in the pumice layer B (at depths between 0.8 and 1.8 m), 20 tensiometers and 11 TDR probes in the deeper layers C1 and C2 (at depths between 2.1 and 2.8 m) [9]. Measurements were collected weekly over two years and are reported in [9]. In this study, field measurements of VWC collected on July 28, 2017 and February 22, 2018, were adopted to validate the geophysical survey carried out on July 29, 2017 and February 24, 2018. Therefore, the dates of the field measurements closest to the two ERT surveys were opted for. Measurements of VWC collected on July 28, 2017 and February 22, 2018 at verticals 1N, 1C and 1S are plotted against depth in Fig. 3a, b. In the dry period, due to evapotranspiration, the volumetric water content was very low in soils A1 and A2, ranging between 0.15 and 0.20, while it attained

higher values in soil C1 (0.40-0.50), which was unaffected by the atmospheric conditions at the soil surface.

Conversely, in February 2018, the VWC increased up to 0.40-0.65 at the top layer because of the persistent rainfall that typically occurs during the wet period. However, the entire VWC profile shifts towards values higher than 0.40 as the rainwater easily infiltrates into the whole soil cover down to the bedrock, as all the layers are characterized by a hydraulic conductivity close to the saturated value.

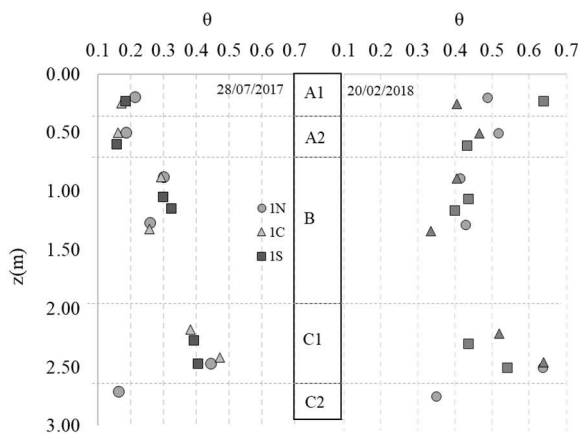


**Fig. 3.** Profiles of field measurements of volumetric water content,  $\theta$ , collected by TDRs at verticals 1N (circle), 1C (triangle) and 1S (square) in Fig. 2b on (a) July 28, 2017 and (b) February 22, 2018 [modified after [1, 9]].

### 3.4 Geophysical investigation

High-resolution 2D and 3D ERT surveys were carried out in the test area along the nine profiles shown in Fig. 2b. The geophysical investigation was devoted to provide, thanks to the integration with the collected geological and geotechnical data, a detailed 3D reconstruction of the investigated buried volume (soil cover and bedrock) in terms of topographic and physical characteristics and saturation degree distribution [1]. In this regard, 3D ERT prospecting was performed on July 29, 2017 (summer) and February 24, 2018 (winter) in order to study the volumetric water content distribution on a seasonal time scale.

An unconventional 3D electrode geometry was used, consisting of three parallel profiles 70.5 m long and spaced 12 m apart (profiles 1, 5 and 9 in Fig. 2b), along which multi-electrode cables with an inter-electrode spacing of 1.5 m were laid. The adopted 3D data acquisition scheme is based on the use of electrodes of each cable as both transmission and measuring devices in order to achieve uniform data coverage within the investigated buried volume (for further details, the reader is referred to [1]).

Figure 4 shows the resistivity sections along the ERT 3 profile (see Fig. 2b), extracted from the 3D resistivity models measured on July 29, 2017 and February 24, 2018. In particular, the pyroclastic cover (approximately 3 m thick) is generally characterized by resistivity ( $\rho$ ) values in the range 90 - 4500  $\Omega\text{m}$  for the two analysed seasonal periods. The top of the bedrock shows

significant variations in the resistivity distribution over the longitudinal development due to a different saturation degree of the uppermost part of the limestone formation ( $\rho$  values in the range 340 - 7000  $\Omega\text{m}$ ). This result suggests that the limestone bedrock is affected by fracture systems and karst filled with the C2 horizon, which favour the accumulation of water, partly due to the rainwater infiltration of the antecedent winter.

With regard to the survey carried out on February 24, both the cover and the underlying bedrock were found, as expected, to be more conductive overall than on July 29, due to the higher rainfall during the wet season. In addition, a different distribution of the resistivity values, both in terms of amplitude and geometry, is observed along the longitudinal slope than that found for the summer survey. In particular, a hydraulic continuity from the top-soil up to the bedrock is very evident; this process can be observed in two/three sectors that play the role of preferential flowpaths. In addition, some of these areas are characterized by the presence of mountain tracks where water can accumulate and easily infiltrate. Finally, this survey also highlights a strong variability in the limestone bedrock, which is characterized by a higher contrast in resistivity values, indicating the presence of more intact and more fractured zones, as well as the presence of a finer-bedded layer of marl interbedded in the calcareous sequence ( $R_m$ ).

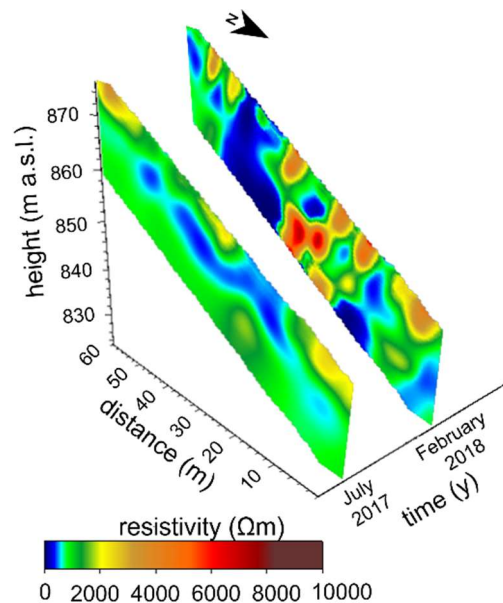


**Fig. 4.** Resistivity sections along profile 3 (see Fig. 2b) extracted from the 3D resistivity models resulting from the July 29, 2017 and February 24, 2018 surveys.

## 4 Integration from geological, geotechnical and geophysical data

### 4.1 2D geological model

To reconstruct the geological model of the investigated slope, the 2D resistivity tomographies were integrated with the geological data from the stratigraphic logs (1N, 1C and 1S in Fig.5). The comparison between

geological and resistivity data allowed the different layers of the pyroclastic cover and the uppermost part of the bedrock to be identified. The stratigraphic details were reproduced at a scale of ten metres along the slope thanks to the ERT model characterized by a resolution of 0.50 m.

The survey carried out in the dry period (July) was used to set up the stratigraphy because, in the absence of significant water content, the electrical signature of each soil horizon can be easily identified. As an example, Fig. 5 shows the geological section reconstructed along profile 3 (see Fig. 2b). The distribution of the resistivity values highlighted a strongly uneven soil cover resting on a bedrock that is highly fractured at the top and more compact at depth. The buried morphology of the bedrock is very complex and characterized by lows and highs due to the karst phenomena ( $R_k$ ). Where the limestones are higher, the soil cover results less thick and usually is observed to lack the B layer.

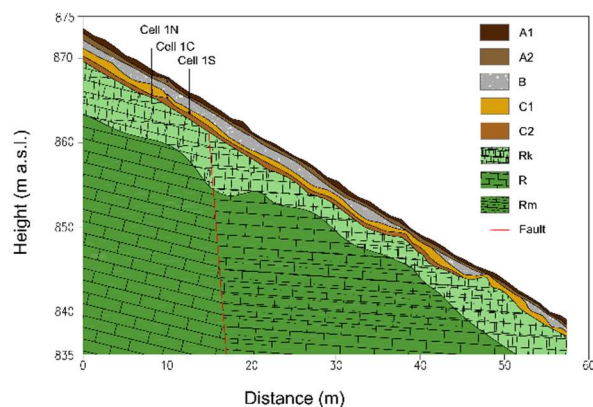


**Fig. 5.** Geological section reconstructed from the 2D ERT images along profiles 3 (see Fig. 2b),  $R_k$  is the karst and fractured limestone bedrock; R is the intact limestone bedrock;  $R_m$  is a marly limestone stratum.

#### 4.2 2D distribution of VWC

To estimate the volumetric water content of the pyroclastic cover, laboratory resistivity tests were carried out on 17 undisturbed soil samples collected from the test site at varying soil water contents. The results of the laboratory measurements and the characteristic  $\rho$  vs.  $S_e$  curves obtained from fitting Archie's law [15] in each pyroclastic layer are reported in [1]. The fitting functions, together with the physical soil properties given in Table 1, were adopted to determine the VWC distribution of the cover along the geological section in Fig. 5. Figures 6a and 6b show the VWC derived from the ERT surveys carried out on July 29, 2017 (summer) and February 24, 2018 (winter) along profile 3, respectively. In particular, low values of volumetric water content, ranging from 0.14 to 0.37, are detected in the first meter of the cover on July 29, 2017 (Fig. 6a). These results are reasonable due to the high evapotranspiration phenomena that occur during the summer. However, in the red-circled area of the cross section in Fig. 6a (at the distance of 44 m), higher VWC are detected in layers B and C1, in correspondence of the section narrowing. The layer C2 is very dry with

VWC ranging between 0.14 and 0.20. As expected, the VWC values observed in the wet season (winter survey, Fig. 6b) are generally higher than those determined on July 29, 2017. Specifically, values between 0.14 and 0.58 are found in the first half of the cover (A1 and A2 layers) and between 0.40 and 0.68 in the lower part (C1 and C2 layers). Notably, the geophysical survey of February 24, 2018 determines volumetric water content values slightly lower than those determined on 29<sup>th</sup> July 2017 at some points in the central part of the section (Fig. 6b, at the black-circled areas). In addition, the distribution of VWCs along the longitudinal slope results more heterogeneous than that found in the summer survey, reflecting the resistivity distribution. All these differences can be realistically justified by variations in the vegetation cover, roots architecture and the understory, which vary seasonally according to the boundary conditions. It is also interesting to note the high volumetric water content detected on 24<sup>th</sup> February 2018 at the bottom of the cover at a distance of 10 m from the beginning of the section (Fig. 6b, at the red-circled area), just in correspondence of the preferential flow path identified in the bedrock in Fig. 4.

To validate the water content distribution determined from the field resistivity surveys by using the fitting functions, the VWCs, measured at fixed points by the TDR measurements [9], were compared with those obtained from the field geophysical investigations at the same depth on the verticals 1N, 1C and 1S, which lie approximately on the ERT section 3 (see Fig. 2b). Table 2 summarizes the VWC values derived from the ERT surveys and the TDR measurements. In general, a fairly good agreement was found; however, some differences were to be expected as the resolution of the geophysical measurements is quite different from that of the geotechnical field measurements presented in this work.

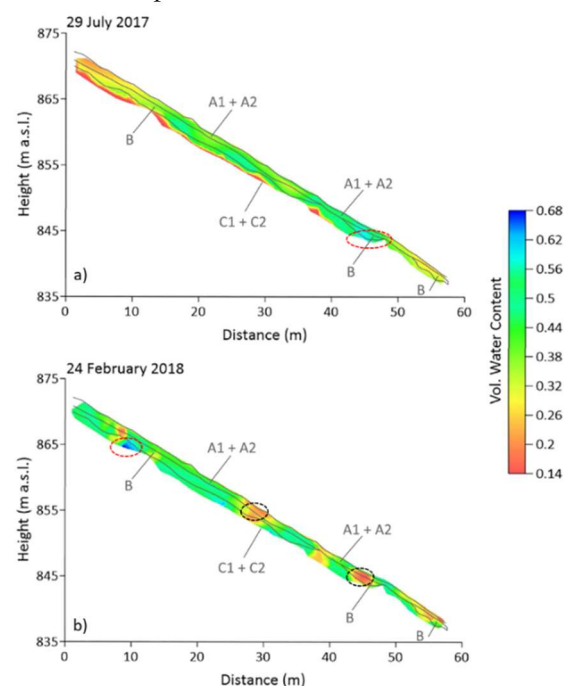


**Fig. 6.** VWC distribution derived from the ERT surveys carried out on July 29, 2017 (a) and February 24, 2018 (b) along profile 3 (see Fig. 2b). The soil layering is overlaid on the profiles.

In this regard, the comparison was not intended to demonstrate a point-by-point match, but aimed to prove that the overall hydraulic behaviour of the slope cover predicted by both geotechnical and geophysical approaches is comparable.

**Table 2.** Volumetric water content,  $\theta_p$ , corresponding to the resistivity values observed along the vertical profiles 1N, 1C, and 1S [9], which lie approximately on the ERT section 3. These values are compared with the volumetric water content provided by TDR measurements,  $\theta_{TDR}$ , for the pyroclastic horizons A1, A2, C1 and C2 on 29<sup>th</sup> July 2017 and 20<sup>th</sup> February 2018.

Soils	Depth (m)	$\theta_p$	$\theta_{TDR}$	$\theta_p$	$\theta_{TDR}$
		07/29/18	07/29/18	02/24/18	02/24/18
1N-A1	0.20	0.25	0.21	0.34	0.459
1N-A2	0.50	0.27	0.18	0.30	0.488
1N-C1	2.47	0.35	0.44	0.32	0.615
1N-C2	2.71	0.22	0.16	0.34	0.35
1C-A1	0.25	0.28	0.17	0.41	0.382
1C-A2	0.50	0.29	0.16	0.54	0.411
1C-C1	2.18	0.26	0.38	0.61	0.506
1C-C1	2.42	0.22	0.47	0.62	0.618
1S-A1	0.23	0.31	0.18	0.39	0.403
1S-A2	0.60	0.32	0.15	0.43	0.405
1S-C1	2.27	0.37	0.39	0.44	-
1S-C1	2.47	0.34	0.40	0.46	0.539

## 5 Conclusion

This paper shows the remarkable potential of combining in situ and laboratory geological, geophysical and geotechnical approaches to achieve a continuous characterization of the stratigraphy and hydrogeological conditions that favour the flow-like landslide occurrence. Detailed information on the local stratigraphy and subsurface of the slope should be properly used in slope stability analysis, as the simplified average slope conditions may not be precautionary.

The proposed procedure has allowed us to move from local information to a virtually continuous picture of the buried slope by identifying local geomorphological irregularities along the slope and their effect on the volumetric water content distribution within the pyroclastic cover. In particular, the interruption of pumices, the narrowing of the pyroclastic cover, the buried morphology of the bedrock and the discontinuities in the finest layer at the bottom have been identified; these features have to be duly taken into account in slope stability analyses.

### Acknowledgements

The present study has been carried out in the framework of the research projects: METROPOLIS (PON ‘Ricerca e Competitività 2007–2013’, Grant No. PON03PE\_00093\_4) and TERRE–H2020–MSCA–ITN 2015 (H2020 “Training Engineers and Researchers to Rethink geotechnical Engineering for a low carbon future”, Grant No. 675762).

The authors acknowledge the support of the present study in the framework of the Cooperation Agreement (coordinated by Prof. Antonio Santo and Prof. Marianna Pirone) between the Department of Civil, Architectural and Environmental

Engineering, University of Naples “Federico II”, Campania Region and ITAL SUD, devoted to the study of the triggering of flow-like landslides within the geological context of the Lattari Mts.

## References

1. R. Di Maio, C. De Paola, G. Forte, E. Piegari, M. Pirone, A. Santo, G. Urciuoli, *Eng. Geol.* **267**(23), 105473 (2020)
2. M. Pirone, R. Papa, M.V. Nicotera, G. Urciuoli *Landslides* **12**(2), 259–276 (2015)
3. M. Pirone, G. Urciuoli, *Cyclical suction characteristics in unsaturated slopes*. In: *Volcanic Rocks and Soils - Proceedings of the International Workshop on Volcanic Rocks and Soils, Ischia, 24–25 Settembre, 2015*, (2016)
4. M. Pirone, R. Papa, M.V. Nicotera, G. Urciuoli. *Analysis of Safety Factor in unsaturated pyroclastic slope*. In: *Landslides and Engineered Slopes Experience*. Theory and Practice, vol. 3, CRC Press, 1647–1654
5. M.M. Crawford, L.S. Bryson, *Eng. Geol.* **233**, 146–159 (2018)
6. S. Rezaei, I. Shooshpasha, H. Rezaei, *Bull. Eng. Geol. Environ.* **78** (5), 3223–3237 (2019)
7. A. Amabile, B. de Carvalho Faria Lima Lopes, A. Pozzato, V. Benes, A. Tarantino, *Phys. Chem. Earth* **120**, 102930 (2020)
8. P. Lehmann, F. Gambazzi, B. Suski, L. Baron, A. Askarnejad, S.M. Springman, K. Holliger, D. Or, *Water Resour. Res.*, **49**, 7992–8004, doi:10.1002/2013WR014560 (2013)
9. A.S. Dias (2019). The effect of vegetation on slope stability of shallow pyroclastic soil covers. PhD Thesis, University of Naples Federico II.
10. A.S. Dias, M. Pirone, M.V. Nicotera, G. Urciuoli, *Geomech. Energy Environ.* **30**, 100235 (2022)
11. A.S. Dias, M. Pirone, M.V. Nicotera, G. Urciuoli, *Acta Geotech.* **17**, 837–855 (2022)
12. G. Di Crescenzo, A. Santo, *Geomorphology* **66**, 255–276 (2005)
13. G. Forte, M. Pirone, A. Santo, M.V. Nicotera, G. Urciuoli, *Eng. Geol.* **257**, 105137 (2019)
14. A. Santo, G. Di Crescenzo, G. Forte, R. Papa, M. Pirone, G. Urciuoli, *Landslides*, **15**(1), 63–82 (2018)
15. G.E. Archie. *Trans. Am. Inst. Min. Metall. Pet. Eng.* 146, 54–62 (1942)